Contribution from the Lash Miller Chemical Laboratories
and Erindale College, University of Toronto, Toronto, Ontario, Canada

Direct Synthesis Using Gold Atoms. Monodioxygen Gold, $Au(O_2)$

D. McINTOSH and G. A. OZIN*

Received February 13, 1976 AIC60115L

The reaction of Au atoms with $^{16}O_2$/Ar mixtures at 10 K yields a single "green" product. Using Au and $^{16}O_2$ concentration experiments, warm-up studies, and $^{16}O_2/^{18}O_2$ and $^{16}O_2/^{16}O^{18}O/^{18}O_2$ isotopic substitution coupled with matrix infrared and uv-visible spectroscopy, the product is characterized to be monodioxygen gold, $Au(O_2)$, having the ligand bonded in a side-on configuration. Extended Hückel molecular orbital calculations proved to be a useful aid toward the assignment of the optical spectrum of $Au(O_2)$. The electronic spectral data for $Au(O_2)$ lead one to believe that the gold-dioxygen bonding interaction in $Au(O_2)$ is more closely akin to the Dewar description of metal-olefin bonding applicable to complexes such as $Ag(C_2H_4)$ and $Au(C_2H_4)$, rather than the extreme case of ion-pair bonding which appears to be an appropriate description for $Ag^+(O_2^-)$.

Introduction

Because it is important to develop a physically and conceptually oriented approach to the subject of dioxygen activation,[1] it is clearly valuable to develop new techniques for generating and studying *unstable* metal-dioxygen complexes and to study the factors controlling side-on and end-on bonding for dioxygen in metal complexes and on surfaces. In this context, the "naked" metal atom is proving to be a useful model for a "coordinatively unsaturated" metal atom in a metal surface[2] and in view of the success of the localized bonding model of chemisorption on metals,[3] one would anticipate that similar molecular and surface dioxygen species might be obtained from isolated metal atoms and atoms aggregated in a metal surface.

Recently it has been discovered that the vapors of Ni, Pd, Pt, Cr, and Cu react with dioxygen under matrix isolation conditions[4,5] to form binary dioxygen complexes of the form $M(O_2)_n$ (where $n = 1$ or 2 for Ni, Pd, or Pt[4] and $n = 2$ for Cr or Cu[5]) in which the O_2 ligands appear to be superoxide in nature. In this paper we describe our findings for the matrix reactions of atomic gold and dioxygen.

Experimental Section

Monatomic gold was generated by either directly heating a thin tungsten rod (0.025 in.) around the center of which was wound gold wire (0.005 in.) or by directly heating a tantalum Knudsen cell (wall thickness 0.015 in., orifice diameter 0.010-0.020 in.), the gold being contained in a boron nitride liner (wall thickness 0.005 in.). The gold metal (99.99%) was supplied by Imperial Smelting Co., Toronto. Research grade $^{16}O_2$ (99.99%) was supplied by Matheson of Canada and $^{16}O_2/^{18}O_2$ and $^{16}O_2/^{16}O^{18}O/^{18}O_2$ isotopic mixtures by Miles Laboratories. The furnace used for the evaporation of the metals has been described previously.[6] The rate of gold atom deposition was continuously monitored using a quartz crystal microbalance.[7] In the infrared experiments, matrices were deposited on either a NaCl or CsI plate cooled to 10 K by means of an Air Products Displex closed-cycle helium refrigerator. Infrared spectra were recorded on a Perkin-Elmer 180 spectrophotometer. Uv-visible spectra were recorded on a standard Unicam S.P. 8000 or Varian Techtron instrument in the range 190-900 nm, the sample being deposited on a NaCl optical plate. Extended Hückel calculations were run on an IBM 370 computer.

Results and Discussion

Infrared Experiments. When Au vapor (which is known to be greater than 99% atomic[8] under the conditions of our experiment) is cocondensed with $^{16}O_2/Ar \simeq 1/10$ matrices (using low concentrations of Au to eliminate complications due to cluster formation,[9] Au:Ar $\simeq 10^{-4}$) at 10 K, a yellowish-green matrix is obtained (Au/Ar and Ar/O_2 matrices under comparable conditions appear colorless). The infrared spectrum of the product (Figure 1A) shows a single absorption at 1091.7 cm^{-1} with a $\Delta\nu_{1/2} \simeq 4$ cm^{-1}. Increasing or decreasing the $^{16}O_2$/Ar ratio from 1/5 to 1/100 produced no evidence of any other species besides the one giving rise to the 1091.7 cm^{-1} absorption. Warming the matrix from 10 to 40 K simply caused a gradual diminution of the absorbance of the 1091.7 cm^{-1} band. The nonobservation of any other absorptions implies that the Au/O_2 matrix reaction yields just a single species. The yellowish-green complex was characterized from $^{16}O_2/^{18}O_2/Ar \simeq 1/1/50$ and $^{16}O_2/^{16}O^{18}O/^{18}O_2/Ar \simeq 1/2/1/100$ isotope substitution experiments (Figures 1B and 1C) to be monodioxygen gold, $Au(O_2)$. The presence of the 1091.7/1029.8 cm^{-1} doublet in the $^{16}O_2/^{18}O_2$/Ar experiment with a 61.9 cm^{-1} isotopic separation (Figure 1B) establishes the presence of a complex containing a single dioxygen ligand. These absorptions are assigned to O-O stretching modes of $Au(^{16}O_2)$ and $Au(^{18}O_2)$, respectively. The absence of a central component in this experiment attributable to $Au(^{16}O^{18}O)$ demonstrates that oxygen dissociation, either on the hot metal source or from reaction with Au atoms, does not occur to any observable extent.

Scrambled $^{16}O_2/^{16}O^{18}O/^{18}O_2$/Ar mixtures were used to gain an insight into the mode of attachment of the dioxygen ligand to the Au atom. The triplet isotope pattern shown in Figure 1C confirms the $Au(O_2)$ assignment. The central component observed at 1060.6 cm^{-1} remained as a single line even with spectral slit widths as low as 0.5 cm^{-1} and clearly belongs to $Au(^{16}O^{18}O)$. The approximately 1/2/1 intensity pattern for this isotopic triplet and the essentially equal $\Delta\nu_{1/2}$ values (4 cm^{-1}) for all three components might be taken as evidence that there is no linkage isomerism for the $Au(^{16}O^{18}O)$ molecule and that the dioxygen ligand is side-on bonded with respect to the gold.[16] This assignment, however, must be treated with caution, as the magnitude of the splitting of the linkage isomers $Au(^{16}O^{18}O)/Au(^{18}O^{16}O)$ could be quite small and for a band roughly 4 cm^{-1} wide might remain unresolved.[5] We therefore recognize that the possibility of end-on bonding in $Au(O_2)$ cannot be dismissed. For the purposes of interpreting the optical data for $Au(O_2)$, we shall assume side-on bonding.

Uv-Visible Experiments. To ensure reproducible conditions, infrared and uv-visible spectra were recorded consecutively from the same $Au(O_2)$ sample in various $O_2/Ar \simeq 1/5$ to 1/50 matrices. The uv-visible spectra were essentially independent of the O_2 concentrations, a typical trace being depicted in Figure 2. Apart from the presence of three sharp absorptions attributable to small amounts of unreacted Au atoms isolated in the Ar matrices[10] at 255, 228, and 225 nm, the spectrum is dominated by an intense, broad ($\Delta\nu_{1/2} \simeq 3260$ cm^{-1}) absorption centered at roughly 423 nm (presumably responsible for the yellowish-green color of $Au(O_2)$). Besides this intense absorption, *three* weaker, high-energy absorptions were observed at roughly 313, 276, and 244 nm. The results of warm-up experiments in the range 10 to 40 K showed a gradual diminution in the absorbances of the four bands at 423, 313, 276, and 244 nm, indicating that they are all associated with a single species, that is, $Au(O_2)$.

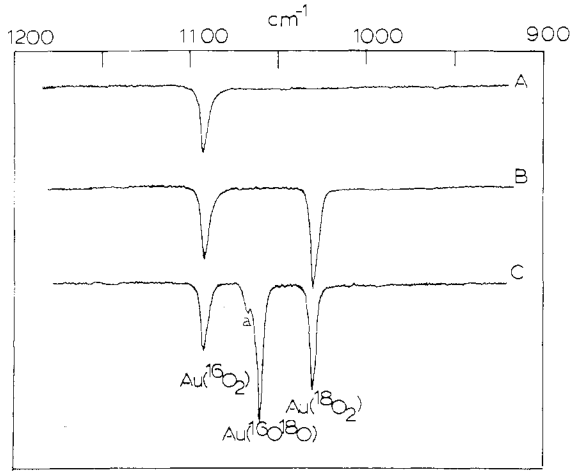

Figure 1. The matrix infrared spectrum observed on depositing Au atoms with (A) $^{16}O_2/Ar \simeq 1/50$, (B) $^{16}O_2/^{18}O_2/Ar \simeq 1/1/100$, and (C) $^{16}O_2/^{16}O^{18}O/^{18}O_2/Ar \simeq 1/2/1/100$ at 10 K. The isotope patterns in the ν_{O-O} stretching region are characteristic of monodioxygen gold, Au(O_2), probably containing a side-on bonded dioxygen ligand (a refers to a matrix site effect).

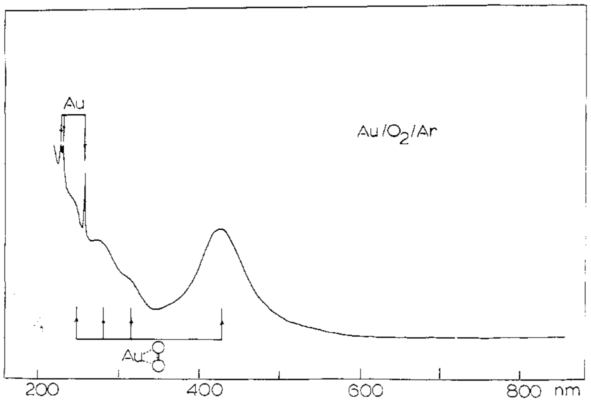

Figure 2. The matrix uv-visible spectrum of the Au($^{16}O_2$) molecule recorded on the same sample described in Figure 1A.

Extended Hückel Molecular Orbital Calculations for Au(O₂). In an effort to obtain an insight into the electronic structure of monodioxygen gold, we have performed extended Hückel molecular orbital calculations on the complex with the C_{2v} geometry shown below:

The close proximity of the ν_{O-O} stretching frequency of Au(O_2) (1091.7 cm^{-1}) to that of free superoxide[11] (1077 cm^{-1}) suggested that the corresponding superoxide O–O internuclear separation (1.34 Å) be used as a starting value in the calculation. As the sums of metal and oxygen covalent radii approximate closely to experimentally determined metal–oxygen internuclear distances in a number of *low oxidation state* transition metal dioxygen complexes,[1] we decided to choose 2.07 Å as a starting value for the Au–O separation.

The basis set of valence atomic orbitals for Au consisted of 5d, 6s, and 6p, and the various orbital exponents and H_{ii} values were taken from the work of Baetzold.[12] The input parameters needed to reproduce our extended Hückel calculation are given in Table I.

The resulting molecular orbital energy level scheme and approximate orbital descriptions for Au(O_2) are shown in Figure 3 and Table II. The main interactions between the gold atom and the dioxygen ligand, as indicated by our calculations, appear to originate from a $O_2(\sigma_g + \pi_u)$ + Au(6s) σ-type donor bond (orbital 3) and a Au ($5d_{xz}$) + $O_2(\pi_g)$ π-type acceptor bond (orbital 6) in Dewar–Chatt–Duncanson terminology.[13]

Table I. Parameters Used in the Calculation of Monodioxygen Gold, Au(O_2)

Gold			Oxygen		
Orbital	Orbital exponent	H_{ii}, eV	Orbital	Orbital exponent	H_{ii}, eV
5d	4.025	−11.09	2s	2.246	−32.33
6s	1.823	−9.22	2p	2.227	−15.80
6p	1.823	−4.37			

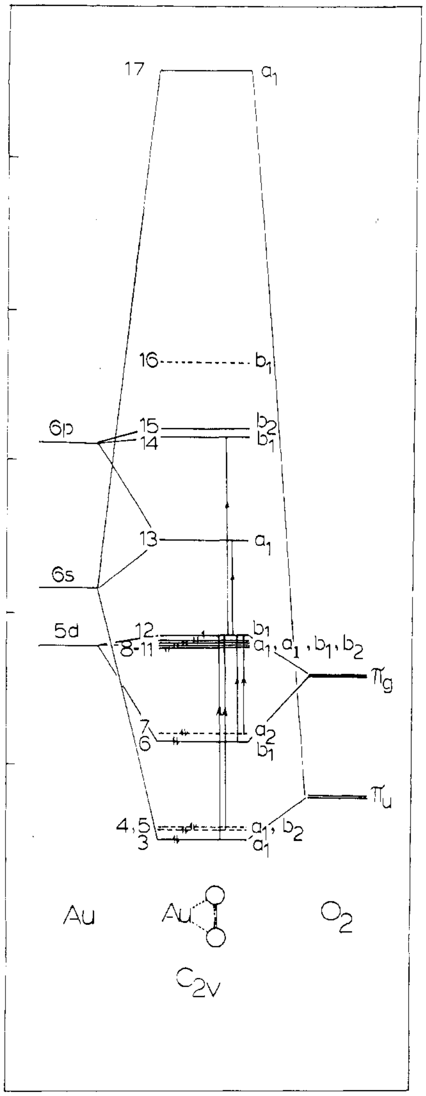

Figure 3. The molecular orbital energy level scheme for Au(O_2) as deduced from extended Hückel calculations (see text for notation). The dotted lines refer to orbitals that are mainly associated with the dioxygen.

The gold atomic orbitals $5d_{x^2-y^2}$, $5d_{xy}$, $5d_{yz}$, and $5d_{z^2}$ remain essentially nonbonding in this scheme (orbitals 8, 9, 10, 11) and lie roughly 3 eV higher in energy than the Au($5d_{xz}$) + $O_2(\pi_g)$ π-bonding molecular orbital 6 referred to above. The unpaired electron resides in a b_1 molecular orbital 12, which is best described as the antibonding counterpart of the Au($5d_{xz}$) + $O_2(\pi_g)$ π-bonding orbital, giving a $^2B_1$ electronic ground state to Au(O_2).

It is conceivable that the visible absorption at 423 nm in the electronic spectrum of Au(O_2) arises from electronic transitions into the partially filled antibonding b_1 level 12 from

Table II. Calculated Orbital Energies for Au(O_2)

Orbital	Symmetry	Energy, eV	Approximate description of orbital[a]	Occupancy
17	a_1	7.91	Au($6sp_z$) – $O_2(\sigma_g + \pi_u)$	0
16	b_1	–1.72	$O_2(\sigma^*p)$	0
15	b_2	–3.99	Au($6p_y$)	0
14	b_1	–4.21	Au($6p_x$)	0
13	a_1	–7.58	Au($6sp_z$)	0
12	b_1	–10.86	Au($5d_{xz}$) – $O_2(\pi_g)$	1
11	a_1	–10.94	Au($5d_{z^2}$)	2
10	b_2	–11.07	Au($5d_{yz}$)	2
9	a_2	–11.08	Au($5d_{xy}$)	2
8	a_1	–11.09	Au($5d_{x^2-y^2}$)	2
7	a_2	–14.05	$O_2(\pi_u)$	2
6	b_1	–14.22	Au($5d_{xz}$) + $O_2(\pi_g)$	2
5	a_1	–17.13	$O_2(\sigma p)$	2
4	b_2	–17.22	$O_2(\pi_g)$	2
3	a_1	–17.40	Au(6s) + $O_2(\sigma_g + \pi_u)$	2
2	b_1	–26.98	$\sigma_s^*(O_2)$	2
1	a_1	–37.41	$\sigma_s(O_2)$	2

[a] Only main contributing atomic orbitals to each molecular orbital are listed, as considerable orbital mixing occurs for Au(O_2) in C_{2v} symmetry. The quoted values refer to the parameters listed in Table I.

either (i) the bonding b_1 Au($5d_{xz}$) + O_2 (π_g) level 6 or (ii) the nearby a_2 π^*O_2 level 7 (both of which are electric dipole and spin allowed (Figure 3)).

On the other hand, a transition from the partially filled b_1 Au($5d_{xz}$) – $O_2(\pi_g)$ level 12 into the upper a_1 Au ($6sp_z$ hybrid type) level 13 could also appear in the visible region and is an equally acceptable assignment for the 423 nm ν_1 absorption.

The three remaining high-energy absorptions at 313, 276, and 244 nm could be associated with the three accessible transitions shown schematically in Figure 3.

While these calculations are qualitatively useful for gaining an insight into the distribution of electronic levels in Au(O_2), we recognize that the absolute transition energies cannot be used with any confidence to distinguish the alternative assignments proposed above.

Discussion

A most intriguing observation relates to the striking similarity in the electronic spectra of

$$\mathrm{Au}\cdots\cdots\begin{matrix}\mathrm{O}\\ \|\\ \mathrm{O}\end{matrix}$$

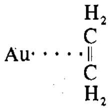

$$\mathrm{Au}\cdots\cdots\begin{matrix}\mathrm{H_2}\\ \mathrm{C}\\ \|\\ \mathrm{C}\\ \mathrm{H_2}\end{matrix}$$

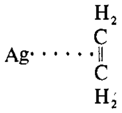

$$\mathrm{Ag}\cdots\cdots\begin{matrix}\mathrm{H_2}\\ \mathrm{C}\\ \|\\ \mathrm{C}\\ \mathrm{H_2}\end{matrix}$$

yet conspicuous dissimilarity to Ag(O_2). Particularly noteworthy is the fact that Ag(O_2) is *colorless*[14] and shows no absorptions above 220 nm, whereas Au(O_2), (C_2H_4)Au, and (C_2H_4)Ag[15] are respectively green, green, and purple. On the basis of the frequencies of their ν_{O-O} stretching modes alone, both Ag(O_2) (1080 cm^{-1}) and Au(O_2) (1092 cm^{-1}) might initially be suspected of being $M^+(O_2^-)$ ion pairs. Although the absence of visible absorptions for Ag(O_2) is consistent with the presence of superoxide and a formally (+1) silver oxidation state, such a bonding description would appear to be untenable for the green complex, Au(O_2).

In view of the fact that the ν_{O-O} stretching frequencies of transition metal dioxygen complexes are not a terribly reliable indicator of the extent of the metal–dioxygen charge transfer,[1] we would like to propose that the gold–dioxygen bonding interaction in Au(O_2) is more closely akin to the Dewar description of metal–olefin bonding applicable to complexes such as (C_2H_4)Au and (C_2H_4)Ag, rather than the extreme case of ion-pair bonding which appears to be an appropriate description for $Ag^+(O_2^-)$. Consistent with these bonding proposals are (i) the substantially lower first ionization potential of Ag (7.57 eV) compared to Au (9.22 eV) and (ii) the *blue*-shifted metal → ethylene π charge transfer transition on passing from (C_2H_4)Ag to (C_2H_4)Au.[15]

Acknowledgment. We gratefully acknowledge the financial assistance of the National Research Council of Canada, the Atkinson Foundation, and Liquid Carbonic. An N.R.C.C. Scholarship for D.M. is also greatly appreciated.

Registry No. Au(O_2), 60294-90-8.

References and Notes

(1) L. Vaska, *Acc. Chem. Res.*, **9**, 175 (1976).
(2) M. Moskovits and G. A. Ozin, "Vibrational Spectra and Structure", J. Durig, Ed., Marcel Dekker, New York, N.Y., 1975; G. A. Ozin, *Acc. Chem. Res.*, in press.
(3) R. Ugo, *Catal. Rev.-Sci. Eng.*, **11**, 225 (1975); E. L. Muetterties, *Bull. Soc. Chim. Belg.*, **84**, 959 (1975).
(4) H. Huber, G. A. Ozin, and A. Vander Voet, *Can. J. Chem.*, **51**, 2722 (1973).
(5) J. H. Darling, M. B. Garton-Sprenger, and J. S. Ogden, *J. Chem. Soc., Faraday Trans. 2*, Symp., 75 (1973).
(6) E. P. Kündig, M. Moskovits, and G. A. Ozin, *J. Mol. Struct.*, **14**, 137 (1972).
(7) M. Moskovits and G. A. Ozin, *J. Appl. Spectrosc.*, (*Engl. Transl.*), **26**, 487 (1972).
(8) M. Ackerman, F. R. Stafford, and J. Drowart, *J. Chem. Phys.*, **33**, 1784 (1960).
(9) E. P. Kündig, M. Moskovits, and G. A. Ozin, *Angew. Chem., Int. Ed. Engl.*, **14**, 292 (1975); and M. Moskovits and G. A. Ozin, "Cryochemistry", Wiley, New York, N.Y., 1976.
(10) D. M. Gruen, S. C. Gandioso, R. L. McBeth, and J. L. Lerner, *J. Chem. Phys.*, **60**, 89 (1974).
(11) J. Rolfe, W. Holzer, W. E. Murphy, and H. J. Bernstein, *J. Chem. Phys.*, **49**, 963 (1968).
(12) R. Baetzold, *J. Chem. Phys.*, **55**, 4355 (1971).
(13) J. Chatt and L. A. Duncanson, *J. Chem. Soc.*, 2939 (1953); M. J. S. Dewar *Bull. Soc. Chim. Fr.*, **18**, C71 (1951).
(14) D. McIntosh and G. A. Ozin, *Inorg. Chem.*, in press.
(15) D. McIntosh and G. A. Ozin, *J. Organomet. Chem.*, in press.
(16) Our experiments indicate that the weak high-frequency shoulder observed at 1068 cm^{-1} on the $^{16}O^{18}O$ stretching mode of Au($^{16}O^{18}O$) at 1060.6 cm^{-1} is best assigned to a matrix site splitting (labeled a in Figure 1C).